Korean J. Chem. Eng., 33(6), 1903-1907 (2016)
DOI: 10.1007/s11814-016-0029-2

pISSN: 0256-1115
eISSN: 1975-7220

Experimental verifications of Mpemba-like behaviors of clathrate hydrates

Yun-Ho Ahn, Hyery Kang, Dong-Yeun Koh, and Huen Lee†

Department of Chemical and Biomolecular Engineering, KAIST, 291 Daehak-ro, Yuseong-gu, Daejeon 34141, Korea
(*Received 3 November 2015 • accepted 25 January 2016*)

Abstract−The exact mechanism of the Mpemba effect of water was recently investigated microscopically and explained on the basis of the cooperative relationship between intramolecular polar-covalent bonds (O-H) and intermolecular hydrogen bonds (O : H). We posited that this relationship might exist in clathrate hydrates since they consist of hydrogen-bonded host water frameworks and enclathrated guest molecules. The formation of tetrahydrofuran (THF) hydrate, which is the simplest clathrate hydrate, was investigated by using differential scanning calorimetry and Raman spectroscopy. THF hydrates show the Mpemba effect at lower initial temperatures, but formation times were delayed at higher initial temperatures because the evaporated THF molecules should be liquefied to correspond to the stoichiometric concentration of guest molecules to form sII clathrate hydrates. However, even though the formation time was delayed at higher initial temperatures, the rates of heat emission during THF hydrate formation, measured in a bulk state, roughly increased as the initial temperature increased. Moreover, we observed that the O : H stretching phonons of water in the THF hydrate showed a blue shift, and the O-H stretching mode showed a redshift as temperature decreased. Both the rate of heat emission and the Raman shift of these two bonds imply that a cooperative relationship between the covalent bond and the hydrogen bond exists in THF hydrate as pure water. The formation kinetics of THF hydrate therefore might depend on its initial temperature, thus showing Mpemba-like behavior.

Keywords: Clathrate Hydrate, THF Hydrate, Mpemba Effect, Initial Temperature, Covalent Bond

INTRODUCTION

The Mpemba effect, named after E. B. Mpemba, is a well-known phenomenon where warmer water freezes faster than colder water [1]. This phenomenon is counterintuitive since the temperature of the warmer water is further from the freezing point than that of the colder water. Even though the freezing rate of water is highly apparatus-dependent in kinetic experiments, several studies have suggested a common result that warmer water freezes faster than colder water [1-6]. This is a verifiable phenomenon, but the exact mechanism of the Mpemba effect has not been revealed clearly. With regard to the mechanism underlying this observation, several possible postulations pointing to the amount of mass lost to evaporation [2]; the amount of dissolved carbon dioxide [3]; the temperature distribution of water (convection currents); and the types and shapes of vessel, gas contents, and impurities [5] have been suggested in the literature as solutions to the Mpemba paradox. Nevertheless, the problem remains unsolved and there has been much controversy.

One interesting study examined the probability of water samples of different temperatures reaching a certain supercooling temperature without freezing through repetitive experiments [4]. Supercooling is a key component of the freezing process since it could be the driving force arranging liquid water molecules into a well-defined order. It also attracts non-ordered liquid water molecules to the initiated nucleus in characteristic locations to form the crystalline structure of ice [6].

Zhang et al. [7] proposed a new microscopic paradigm wherein the Mpemba effect could be explained based on the relationship between intramolecular polar-covalent bonds (O-H) and intermolecular hydrogen bonds (O : H). Prior to their research, Sun et al. [8] proposed a cooperative blue shift of O : H stretching phonons and a red shift of the O-H stretching mode during the cooling process through Raman measurements and MD calculations. The corresponding research indicates that the cooling process first shortens and stiffens the intermolecular hydrogen bonds, and then lengthens and softens intramolecular covalent bonds. Huang et al. [9] also suggested an H-bridged oscillator model composed of two asymmetric, coupled hydrogen and covalent bonds. They showed that the Coulomb repulsion between electron pairs on adjacent oxygen atoms depends on the O-O distance. Moreover, they were able to show that, to minimize their potentials, both hydrogen and covalent bonds change their length during cooling and heating processes along potential curves. Based on these previous studies, Zhang et al. [7] concluded that the cooling process first shortens the hydrogen bond, and then sequentially lengthens the covalent bond with the emission of entrapped energy. At this point, the amount of entrapped energy, the change of contracted O-H bond length, and the rate of energy release are proportional to the initial temperature of the system. Through such findings, we can explain the Mpemba effect with microscopic experimental and computational analyses: the warmer water freezes faster due to the rapid emission of entrapped energy in its covalent bonds.

Clathrate hydrates are ice-like crystalline solids, and small guest

†To whom correspondence should be addressed.
E-mail: hlee@kaist.ac.kr
‡This article is dedicated to Prof. Huen Lee on the occasion of his retirement from KAIST.

molecules can be enclathrated inside cages of hydrogen-bonded water frameworks within them [10]. The hydrate formation process consists of (1) the formation of nuclei, (2) growth of nuclei at a liquid-liquid or liquid-gas interface, (3) diffusion of components to the growing hydrate surface, and (4) dissipation of heat of crystal formation [11,12]. Since a range of guest molecules with varying sizes can be captured in the hydrogen-bond cages, and each guest molecule causes different magnitudes of repulsion between itself and the hydrogen-bonded host framework, we observe considerable structural flexibility with clathrate hydrates. Such characteristics regarding structural flexibility can be exploited for applications such as hydrogen storage with a tuning phenomenon [13] or multiple hydrogen storage in a single small cage [14].

Among the several possible guest molecules, tetrahydrofuran (THF) is one of the well-known sII hydrate formers with a self-forming effect that does not require the help of gas molecules, and it can independently fill the large cages of sII hydrate [15]. Hence, THF hydrate is the simplest system among the clathrate hydrates. The miscibility of THF with water makes it possible to form hydrate crystals at the liquid-liquid interface, and thus THF hydrate does not require high pressure, in contrast to gas hydrates. Moreover, it reduces the gas hydrate formation pressures (or increases temperatures), resulting in enhanced kinetics of hydrate formation [16]. For practical engineering applications involving gas storage and separation processes, the thermodynamic equilibrium and kinetics of THF hydrate formation with gas mixtures have been intensively studied [16,17]. Fundamental research regarding kinetic hydrate inhibitors, especially important issues in flow-assurance fields, has been carried out using THF hydrate systems [18,19]. However, the kinetics of the hydrate formation rate depending on the initial temperature of the system has not been studied yet. Since the clathrate hydrates have a unique hydrogen-bonded water framework structure, and the Mpemba effect could take place even with solutions or other liquids [6], the hydrate formation rate also might be dependent on the initial temperature, showing the Mpemba effect. Therefore, in this study, using a differential scanning calorimetry, we examined the kinetics of THF hydrate formation with respect to the initial temperature and compared it with that of water/ice. Moreover, using Raman spectroscopy, we also examined the changes of hydrogen and covalent bonds of THF hydrates with various temperatures.

EXPERIMENTAL SECTION

1. Materials and Sample Preparation

Deionized water of ultrahigh purity was supplied by Merck (Germany) and tetrahydrofuran (THF) was supplied by Sigma-Aldrich Inc. The 0.0556 mole fraction of THF corresponds to the stoichiometric amount of water for the sII hydrate ($THF{\cdot}17H_2O$), but slightly larger amounts of THF (0.06 mole fraction) solutions were used to minimize the amount of unconverted water.

2. Differential Scanning Calorimetry Analyses

An ultra-low temperature differential scanning calorimeter (DSC 214 Polyma, Netzsch, Germany) with a resolution of 0.1 μW and a cooling system that operates down to 103 K using liquid nitrogen was used to measure the freezing time and temperature of water and the formation time and temperature of THF hydrate. Amounts and rates of heat emission during the structure transition from water to ice or from THF solution to THF hydrate were also measured. Before the experiments, the temperature and heat sensing of DSC were calibrated with indium for precise measurements. After calibration, approximately 20 mg of a liquid sample (water or THF solution) was loaded in the aluminum pan, and the aluminum lid closing the pan was pressurized by a sealing press to facilitate a closed system. This sample holder can endure a pressure of up to 3 bar, and hence it can be assumed that there is no loss of sample caused by evaporation. As shown in Fig. 1, the heating and cooling system of DSC controls the temperature profile (black solid line) as follows: (1) keep the initial temperature around 20 min to reach equilibrium, (2) lower the temperature with a constant cooling rate of −5 K/min to 243 K (to obtain plenty of data with a proper freezing or formation time scale, the optimized cooling rate was chosen), (3) keep at 243 K for 3 minutes, and (4) raise the temperature at a constant heating rate of 3 K/min up to room temperature. During the cooling process from the initial temperature to 243 K, an exothermic peak was observed due to heat emission from the formation of hydrate crystals (or ice freezing). Conversely, during the heating process from 243 K to room temperature, an endothermic peak was observed due to the hydrate dissociation (or ice melting). The same experiment was repeated eight times for each initial temperature with a new sample. The definition of the 'formation time of THF hydrates' in the context of this experiment is the time measured from the moment the sample's temperature reaches 278 K until the formation of hydrate crystals with an exothermic peak. Similarly, the 'formation temperature of THF hydrates' can be also defined as the temperature when hydrate formation starts, as shown in Fig. 1.

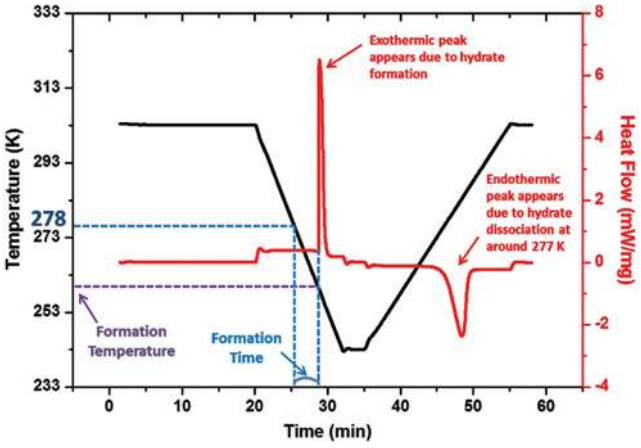

Fig. 1. Temperature and heat flow profiles with four steps (constant initial temperature, cooling, constant temperature of 243 K, and heating) controlled by a differential scanning calorimeter. Exo- and endothermic peaks were measured with hydrate formation and dissociation, respectively. Hydrate formation time and temperature could be obtained as shown above.

3. Raman Analyses

The Raman spectra were obtained using a Horiba Jobin Yvon LabRAM HR UV/Vis/NIR high-resolution dispersive Raman microscope. A focused 514.53 nm line of an Ar ion laser was used as an

excitation source, and its typical intensity was 30 mW. The scattered light was dispersed using an 1800 grating of a spectrometer and was detected by a CCD detector with electrical cooling (203 K). For the various temperature experiments, a Linkam (THMS600G) unit was used to control the sample temperature. At each temperature, sufficient time was provided to reach the equilibrium state.

RESULTS AND DISCUSSION

First, it was necessary to check whether the differential scanning calorimeter could observe the Mpemba effect of the water during freezing process. To this end, the freezing time of water was measured with various initial temperatures ranging from 283 K to 353 K. As discussed in the experimental section, the freezing time of water was defined as the time from when the sample's temperature reached 278 K until the structure transition occurred. Fig. 2(a) represents the average freezing time of water plotted with respect to the initial temperature, showing one standard deviation from the mean of repetitive experiments for each initial temperature. A second-order polynomial function can be fitted to this graph, and the trend is similar with results reported in the literature [7].

Since the amount of water is different from that in the experiments in the literature, the time scale was quite small. However, the trend where freezing time becomes inversely proportional to the initial temperature from 293 K was reproduced and confirmed by the differential scanning calorimetry results. Moreover, the freezing temperature of water was also measured and plotted, as shown in Fig. 2(c). As the cooling rate of −5 K/min remained constant, the freezing temperature was inversely proportional to the freezing time and proportional to the initial temperature of water. After confirming the occurrence of the Mpemba effect in water using a differential scanning calorimeter, the formation of THF hydrate was investigated.

The THF hydrate formation followed the process shown in Fig. 1. During the cooling process, an exothermic peak was observed due to the formation of THF hydrates. Conversely, an endothermic peak was observed at about 277 K, the dissociation point of the THF hydrate. The formation time (Fig. 2(b)) and temperature (Fig. 2(d)) of THF hydrate correspond with the Mpemba effect of water when initial temperatures are low, but differ when initial temperatures are high. Forming hydrate structures at 293 K with initial temperature ranging from 278 K to 318 K takes the greatest

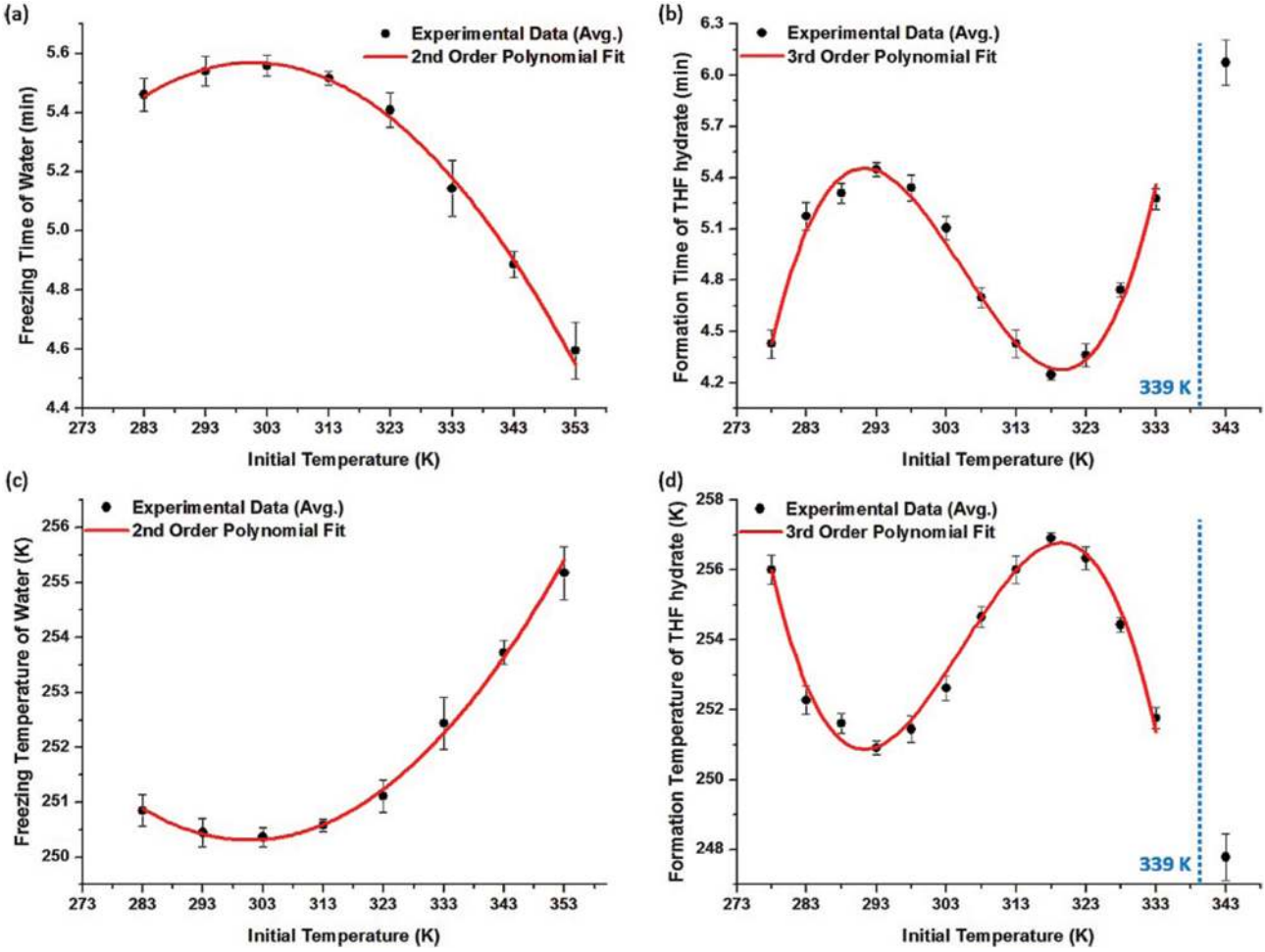

Fig. 2. (a) The average freezing time and (c) temperature of water fitted with second-order polynomial curves. (b) The average formation time and (d) temperature of THF hydrate fitted with third-order polynomial curves. The error bars are indicated on averaged lines with one standard deviation.

amount of time, and the formation time decreases as the initial temperature of THF solution increases. However, when the initial temperature is higher than 318 K, the formation time continues to increase with respect to the initial temperature and best fits to a third-order polynomial function, as shown in Figs. 2(b) and (d).

This discordance can be explained based on the higher level of complexity and differences between THF hydrate structure formation and ice formation. In the case of ice formation, non-ordered water molecules are attracted to the nucleus, and hydrogen bonds are then formed between the nucleus and non-bonded water molecules [6]. However, in the case of THF hydrate formation, non-ordered water molecules and THF molecules are both attracted to the nucleus and enclathrated by neighboring ordered water frameworks. To form structure II hydrates, the stoichiometric 5.56 mol% concentration of guest molecules for the complete occupation of $5^{12}6^4$ cavities should be satisfied [10]. From this molecular point of view, THF molecules tend to start evaporating into a gas phase, with this tendency growing stronger as the initial temperature increases beyond 318 K and approaches the boiling point of 339 K. Therefore, some evaporated THF molecules must be re-liquefied at the gas-liquid interface in order to be diffused to clathrate hydrate nuclei to form THF hydrate structures, causing disharmony with the Mpemba effect. On the other hand, pure water which remains in liquid phase at high temperature could freeze without some evaporated water molecules since the ice structure does not need to satisfy the stoichiometry. Hence, the longest formation time was recorded for THF hydrates when the initial temperature of the THF solution was higher than the boiling point of THF (343 K) because all evaporated THF molecules must be liquefied before the formation could occur.

During the formation processes, we can obtain both the amount and the rate of heat emission during the structure transition (ice freezing and THF hydrate formation) using the heat flow data. As shown in Fig. 1, the rate of heat emission can be obtained with heat flow values when the structure transition occurs. Moreover, we can integrate the heat flow profile with respect to time and obtain the total amounts of heat during the structure transition. The amounts of heat emission are around 300 (J/g) during the water to ice transition, and around 200 (J/g) during THF hydrate formation regardless of their initial temperatures, as shown in Fig. 3(a). The rates of heat emission during the water to ice transition and during THF hydrate formation roughly increase as the initial temperature increases, as shown in Fig. 3(b). Even though the amount and the rate of heat release from O-H covalent bonds are proportional to the initial temperature of the system [7], only the rates of heat emission show increases for both water and THF hydrate since they are measured in a bulk state. In particular, the covalent bonds of water in the hydrate phase might be influenced by the unique guest-host interaction of the clathrate hydrate, and consequently the amounts and rates of heat emission shown do not solely originate from the covalent bonds. We can analyze both the amounts and rates of heat emission for water and the THF hydrate system macroscopically by using a differential scanning calorimeter, but the results are somewhat different from the results from microscopic studies in the literature [7-9].

To investigate the cooperative relationship between the intramolecular polar-covalent bonds (O-H) and intermolecular hydrogen bonds (O : H) for the THF hydrate system, Raman spectra were measured with various temperatures from 218 K to 293 K. Raman shifts similar to that of water [7-9] - two cooperative bonds of a H-bridged oscillator model - were observed. First, as shown in Fig. 4, the ring breathing mode of THF in both hydrate and solution phases (920 cm^{-1}, [10]) was observed and remained constant regardless of the temperature. Above the dissociation point of THF hydrate, the C-O-C stretching mode in solution phase (892 cm^{-1}, [10]) was observed and also remained constant. However, similar to pure water, O : H stretching phonons of water in the THF hydrate system showed a blue shift from 206 to 219 cm^{-1}, and the O-H stretching mode showed a red shift from 3,160 to 3,129 cm^{-1} as the temperature decreased from 273 to 218 K. Above 277 K, the shift of O:H stretching phonons was not clearly detected, and thus we could not compare it with existing data in the literature. Although according to the literature [8] the Raman peak of O : H stretching phonons of water appears at around 75 cm^{-1}, we limited our analysis of the Raman spectra to only around 100 cm^{-1} due to equipment limitations. The Raman peak of the O-H stretching mode appears broadly

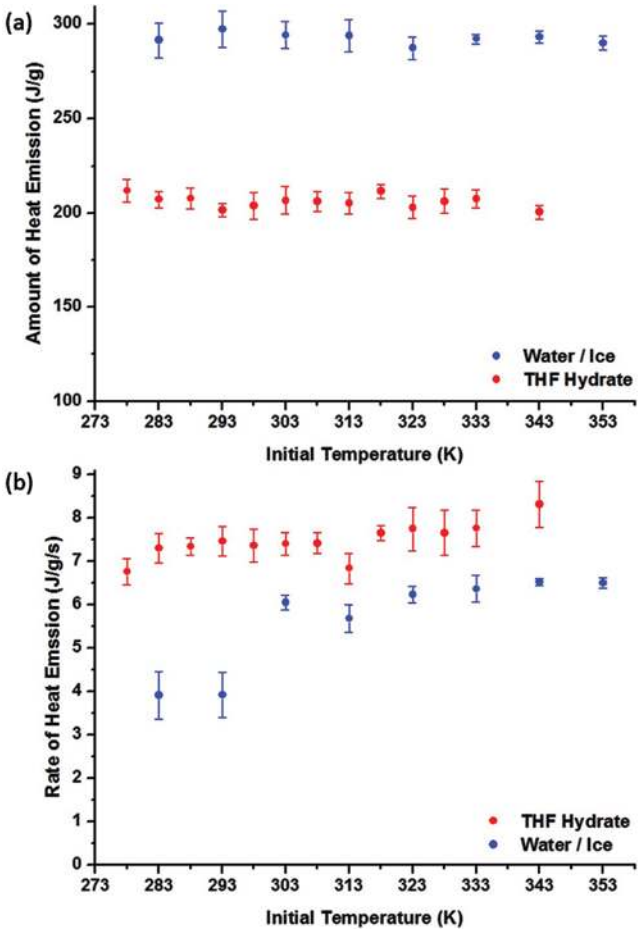

Fig. 3. (a) The amount and (b) the rate of heat emission during both water to ice transition and THF hydrate formation. As the initial temperature increases, the amount of heat emission remains constant but the rate of heat emission roughly increases.

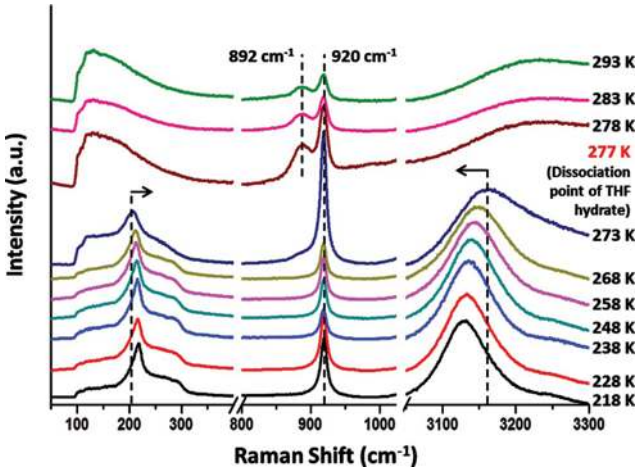

Fig. 4. Raman spectra of THF hydrate measured at various temperatures. The stretching phonons of hydrogen bonds and the stretching mode of covalent bonds show a blue shift and a red shift, respectively, as temperature decreases.

from 293 to 278 K, showing a small red shift. The Raman spectra of the THF hydrate with various temperatures show reverse-shifts of O : H stretching phonons and O-H stretching mode, pointing to the cooperative relationship of two bonds, like a pure water system. Therefore, the relationship of the two bonds can be said to be the main cause of the Mpemba-like behavior in the formation of the THF hydrate.

CONCLUSION

We investigated the formation process of THF hydrate to verify whether the kinetics of THF hydrate formation depends on the initial temperature. When the initial temperature is in a range from 278 to 318 K, THF solutions display the same Mpemba effect as water, where warmer solutions form hydrates faster than colder solutions. However, at initial temperature above this range (above 318 K), the formation time is delayed, because close to 339 K, some THF molecules exist in gas form and evaporated THF molecules must be liquefied before they form hydrate structures. However, once the stoichiometric concentration for sII hydrate is satisfied, the hydrate formation occurs with a faster rate of heat emission, as confirmed by heat flow measurement with a differential scanning calorimeter. As THF hydrate consists of hydrogen-bonded water molecules, like the structure of ice, a cooperative relationship between the intramolecular polar-covalent bonds (O-H) and intermolecular hydrogen bonds (O : H) is also confirmed using Raman spectroscopy. As with water, the cooling process shortens and stiffens the hydrogen bonds but lengthens and softens the covalent bonds, as detected through the blue shift and red shift of the Raman peak, respectively. Therefore, we can conclude that THF hydrates show Mpemba-like behavior during their formation, and this characteristic should be taken into consideration when investigating the kinetics of hydrate formation.

ACKNOWLEDGEMENTS

This research was funded by the Ministry of Trade, Industry & Energy (MOTIE) through the "Recovery of Natural Gas Hydrate in Deep-Sea Sediments Using Carbon Dioxide and Nitrogen Injection" project [KIGAM-Gas Hydrate R&D Organization]. It was also supported by the Midcareer Researcher Program through a National Research Foundation Korea (NRF) grant funded by the Ministry of Science, ICT and Future Planning (MSIP) (NRF-2014-049237).

REFERENCES

1. E. B. Mpemba and D. G. Osborne, *Phys. Educ.*, **14**, 172 (1979).
2. G. S. Kell, *Am. J. Phys.*, **37**, 564 (1969).
3. M. Freeman, *Phys. Educ.*, **14**, 417 (1979).
4. D. Auerbach, *Am. J. Phys.*, **63**, 882 (1995).
5. M. Jeng, *Am. J. Phys.*, **74**, 514 (2006).
6. S. Esposito, R. De Risi and L. Somma, *Phys. A*, **387**, 757 (2008).
7. X. Zhang, Y. Huang, Z. Ma and C. Q. Sun, O : H-O Bond Anomalous Relaxation Resolving Mpemba Paradox (2013), DOI:10.1039/C4CP03669G.
8. C. Q. Sun, X. Zhang, X. J. Fu, W. T. Zheng, J. L. Kuo, Y. C. Zhou, Z. X. Shen and J. Zhou, *J. Phys. Chem. Lett.*, **4**, 3238 (2013).
9. Y. L. Huang, Z. S. Ma, X. Zhang, G. H. Zhou, Y. C. Zhou and C. Q. Sun, *J. Phys. Chem. B*, **117**, 13639 (2013).
10. E. D. Sloan and C. A. Koh, Clathrate Hydrates of Natural Gases CRC Press (2008).
11. P. Bollavaram, S. Devarakonda, M. S. Selim and E. D. Sloan, *Ann. Ny. Acad. Sci.*, **912**, 533 (2000).
12. H. Ganji, M. Manteghian and K. S. Zadeh, *J. Chem. Eng. Jpn.*, **39**, 401 (2006).
13. H. Lee, J. W. Lee, D. Y. Kim, J. Park, Y. T. Seo, H. Zeng, I. L. Moudrakovski, C. I. Ratcliffe and J. A. Ripmeester, *Nature*, **434**, 743 (2005).
14. D. Y. Koh, H. Kang, J. Jeon, Y. H. Ahn, Y. Park, H. Kim and H. Lee, *J. Phys. Chem. C*, **118**, 3324 (2014).
15. S. R. Gough and D. W. Davidson, *Can. J. Chem.*, **49**, 2691 (1971).
16. P. Linga, A. Adeyemo and P. Englezos, *Environ. Sci. Technol.*, **42**, 315 (2008).
17. A. Eslamimanesh, A. H. Mohammadi, D. Richon, P. Naidoo and D. Ramjugernath, *J. Chem. Thermodyn.*, **46**, 62 (2012).
18. H. Zeng, L. D. Wilson, V. K. Walker and J. A. Ripmeester, *J. Am. Chem. Soc.*, **128**, 2844 (2006).
19. H. Kang, D. Y. Koh, Y. H. Ahn, S. Jung, J. Park, J. Lee and H. Lee, *J. Chem. Eng. Data*, **60**, 238 (2015).